

Received 14 June 2019; revised 16 July 2019; accepted 21 July 2019. Date of publication 29 July 2019; date of current version 6 December 2019. The review of this paper was arranged by Editor M. Lemme.

Digital Object Identifier 10.1109/JEDS.2019.2931614

Flexible IGZO TFTs and Their Suitability for Space Applications

JÚLIO C. COSTA¹, ARASH POURYAZDAN¹, JULIANNA PANIDI², FILIPPO SPINA¹ (Student Member, IEEE), THOMAS D. ANTHOPOULOS^{2,3}, MACIEJ O. LIEDKE⁴, CHRISTOF SCHNEIDER⁴, ANDREAS WAGNER⁴, AND NIKO MÜNZENRIEDER^{1,5} (Member, IEEE)

¹ Flexible Electronics Laboratory, Sensor Technology Research Centre, University of Sussex, Brighton BN19QT, U.K.

² Department of Physics, Imperial College London, London SW7 2AZ, U.K.

³ Physical Science and Engineering Division, King Abdullah University of Science and Technology, Thuwal 23955-6900, Saudi Arabia

⁴ Nuclear Physics Division, Helmholtz-Zentrum Dresden-Rossendorf, 01328 Dresden, Germany

⁵ Faculty of Science and Technology, Free University of Bozen-Bolzano, 39100 Bolzano, Italy

CORRESPONDING AUTHOR: J. C. COSTA (e-mail: jc711@sussex.ac.uk)

This work was supported in part by the Engineering and Physical Sciences Research Council, in part by the Global Challenges Research Fund, and in part by the National Institute for Health Research under Grant EP/R013837/1 (SmartSensOtics).

ABSTRACT In this paper, low earth orbit radiation (LEO), temperature, and magnetic field conditions are mimicked to investigate the suitability of flexible InGaZnO transistors for lightweight space wearables. More specifically, the impacts of high energetic electron irradiation with fluences up to 10^{12} e^-/cm^2 , low operating temperatures down to 78 K and magnetic fields up to 11 mT are investigated. This simulates 278 h in LEO. The threshold voltage and mobility of transistors that were exposed to e^- irradiation are found to shift by $+(0.09 \pm 0.05)$ V and $-(0.6 \pm 0.5)$ $\text{cm}^2\text{V}^{-1}\text{s}^{-1}$. Subsequent low temperature exposure resulted in additional shifts of $+0.38$ V and -5.95 $\text{cm}^2\text{V}^{-1}\text{s}^{-1}$ for the same parameters. These values are larger than the ones obtained from non-irradiated reference samples. Conversely, the performance of the devices was observed not to be significantly affected by the magnetic fields. Finally, a Cascode amplifier presenting a voltage gain of 10.3 dB and a cutoff frequency of 1.2 kHz is demonstrated after the sample had been irradiated, cooled down, and exposed to the magnetic fields. If these notions are considered during the systems design, these devices can be used to unobtrusively integrate sensor systems into space suits.

INDEX TERMS Flexible electronics, space applications, amorphous oxides, wearables, thin film transistors.

I. INTRODUCTION

The development of electronic devices for space applications is a widely researched topic since the beginning of the space age. Due to the extreme conditions present outside the Earth's atmosphere, specialized electronic equipment and shielding are required to make these devices capable of withstanding conditions such as large temperature variations, or constant doses of radiation. As an example, special considerations have to be taken when developing instrumentation for the International Space Station, as it regularly passes through the South Atlantic Anomaly (SAA) [1]. This area is characterised by an increase in radiation and energized charged particles due to the weak local geomagnetic field - in particular, the flux of energized electrons

(energies up to 5 MeV) can reach 10^6 $e^-/\text{cm}^2\text{s}$ [2], [3]. The interaction between these electrons and electronic systems causes failures due to ionization effects and atomic displacements in the bulk of semiconductors, which has been prevented by the implementation of bulky shielding structures. As space travels become more common and more sensors are used to ensure the astronauts safety, the development of lightweight and robust electronic devices is required. In this context, flexible electronics are a viable option for the development of future space suits. Fig. 1 shows a vision for spacesuit integrated textile electronics. Various materials compatible with thin film technologies have been tested for space applications, including organic semiconductors such as pentacene and hydrogenated amorphous silicon (a-Si:H).

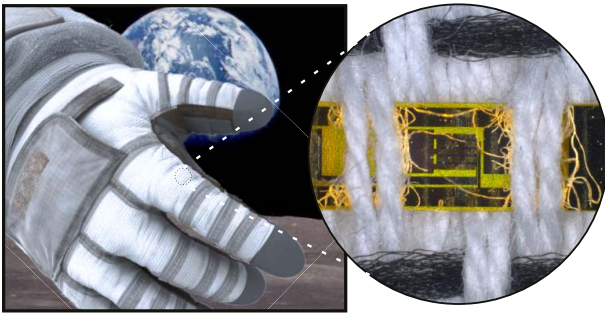


FIGURE 1. Concept of an a-IGZO circuit incorporated into a spacesuit. This material could be used for the development of unobtrusive sensor systems that measure, e.g., temperature and radiation.

However, organic materials were observed to be unstable in conditions similar to the ones found in space [4]. Simultaneously, a-Si:H presents a stable response under outer space conditions but has a relatively low mobility ($\approx 1 \text{ cm}^2 \text{ V}^{-1} \text{ s}^{-1}$) [5]. For these reasons, alternative materials compatible with flexible technologies should be studied for space applications. Amorphous oxide materials such as Indium Gallium Zinc Oxide (a-IGZO) [6] are adequate candidates for the development of conformable and lightweight, yet high performance, sensor systems [7]. Additionally, its amorphous phase improves its radiation hardness since there is no crystalline structure to be damaged. To apply this semiconductor to space wearable applications, its suitability and stability must be assessed. While the electric stability of amorphous oxide semiconductor devices represents an open research question, this topic is also widely studied by numerous groups [8], [9]. Similarly, the mechanical stability of a-IGZO has already been extensively studied by demonstrating outstanding bending stability down to $25 \mu\text{m}$ bending radii [10], [11], [12], [13]. However, additional potential deterioration mechanisms including low temperature, magnetic field and electron irradiation stress are equally important for space applications. Previously, it was shown that rigid a-IGZO transistors continue to operate after being exposed to relatively low energetic electron irradiation (0.8 MeV , $10^{14} \text{ e}^-/\text{cm}^2$) [14]. Nevertheless, the employed bulky and rigid substrates can shield and interact with the semiconductor channel [15], [16]. Simultaneously, the electrons in the SAA are more energetic. Hence, these results cannot be used to predict the response of devices on thin flexible polymeric substrates. Furthermore, in order to preserve conformability, flexible a-IGZO TFT based systems cannot be shielded with bulky glass or lead encapsulations. Similarly, it is known that a-IGZO can function at low temperatures, more specifically, a-IGZO TFTs on glass were shown to remain operational down to 10 K [17]. However, due to the larger thermal expansion of deformable polymer foils (20×10^{-6}) [18] compared to rigid substrates such as glass (-1×10^{-6}) [19] at cryogenic temperatures, it is necessary to characterize the temperature stability of flexible a-IGZO thin film transistors (TFTs) [20]. In addition,

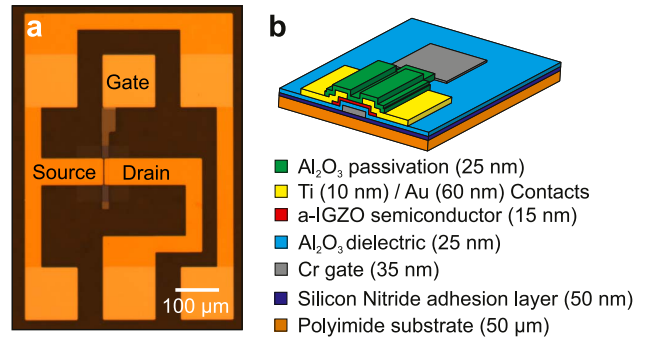


FIGURE 2. a) Micrograph of the transistors studied in this work. b) Schematic of the staggered bottom gate transistors.

a-IGZO TFTs on glass have also been shown to present a magnetoresistive effect [21]. This effect was attributed to the properties of the employed gate insulator materials. More specifically, it was proposed that using SiO_x or SiN_x led to a magnetoresistive effect arising from the paramagnetic and diamagnetic properties of oxygen and nitrogen, respectively [21]. Al_2O_3 is another dielectric which is commonly employed as a gate insulator in a-IGZO TFTs due to the high-quality interface between the two materials. However, until now it was not clear if Al_2O_3 has the same effect as SiN_x or SiO_x . Therefore, in this work, we assess the performance of flexible a-IGZO TFTs that use Al_2O_3 as the gate insulator under various magnetic fields.

Here, the effects of four separate stressing conditions on the electrical characteristics of flexible a-IGZO transistors are assessed. Initially, they are characterised before and after exposure to electrons with an energy of 34.1 MeV and electron fluences spanning 6 orders of magnitude. Afterwards, the devices were characterised at temperatures down to 78 K , which is below the minimum temperature measured for shaded objects in Low Earth Orbit (LEO) [22]. The operation of these devices when exposed to magnetic fields up to 11 mT was then studied, and finally the same devices were tested under bending stress. It is demonstrated that these flexible devices remained fully operational and were not significantly affected after being irradiated by 34.1 MeV electrons with an electron density of $10^{12} \text{ e}^-/\text{cm}^2$, followed by the exposure to 78 K and also under the influence of magnetic fields. These measurements simulate a 278 h spacewalk above the South Atlantic Anomaly, which is sufficiently longer than typical spacewalks. Finally, the operation of a flexible Cascode amplifier is demonstrated after the sample was exposed to the aforementioned conditions. The demonstration of this circuit indicates that more complex circuits and systems based on flexible a-IGZO TFTs have the potential to be implemented in space applications.

II. DEVICE FABRICATION

Fig. 2a shows a micrograph of a representative transistor sample characterised here. The IGZO TFTs were fabricated on a free standing $50 \mu\text{m}$ thick polyimide foil (Fig. 2b)

using conventional UV lithography [23]. To improve adhesion and to prevent outgassing of the substrate, a 50 nm thick silicon nitride layer was deposited on both sides of the substrate using plasma enhanced chemical vapor deposition. The gate consists of a 35 nm-thick Cr layer deposited through e-beam evaporation. The 25 nm-thick Al_2O_3 gate insulator layer was deposited through atomic layer deposition (ALD) at a temperature of 150 °C. This represents the highest process temperature involved into the fabrication process. Afterwards, a 15 nm-thick amorphous IGZO layer was deposited by radio frequency magnetron sputtering at room temperature. The gate, gate insulator, and semiconductor layers were structured by wet etching. The drain and source contacts were fabricated in a lift-off process by depositing 10 nm of titanium and 60 nm of gold through e-beam evaporation. The subsequent ALD deposition and structuring of an additional 25 nm-thick Al_2O_3 layer passivated the transistors and concluded the fabrication process.

III. RESULTS AND DISCUSSION

The devices were measured using a Keysight B1500A parameter analyser. Electron irradiation was performed at a direct-beam end-station at the superconducting electron LINAC ELBE [24] at Helmholtz-Zentrum Dresden-Rossendorf (HZDR) in standard atmosphere. The electron fluence calibration has been performed by measuring the electric current in a Faraday cup and the dose rate in an ionization chamber Roos model 34001 [25]. We assume an error of the fluence measurement of max. $\pm 10\%$. Furthermore, the penetration depth for high energy electrons is in the range of centimetres, and as such the 25 nm-thick Al_2O_3 passivation layer is not able to effectively shield the semiconductor channel [26]. Electrical characterisation of the devices at low temperatures was carried out under vacuum (1×10^{-5} mbar) at temperatures varying from 78 K to 310 K using a cryogenic probe station (Janis Research, ST-500) and an Agilent B2902A source measure unit. The low temperature measurements were conducted in vacuum as even in inert atmospheres the residual air humidity would condense on the surface of the devices and hinder their proper characterisation. In addition, all measurements were conducted in the dark, using transistors originating from the same substrate. Performance parameters were extracted from the saturation regime using the Shichman-Hodges model [27].

A. TRANSISTOR PERFORMANCE

Fig. 3 shows the normalised and averaged transfer and output curves of 75 individual TFTs. From the saturation transfer curve (Fig. 3a), an average threshold voltage (V_{th}) of 0 V, a field effect mobility (μ_{FE}) of $12 \text{ cm}^2 \text{ V}^{-1} \text{ s}^{-1}$, a subthreshold swing (S) of 233 mV/dec, a I_{ON}/I_{OFF} ratio $> 10^7$, and a maximum transconductance g_m ($V_{GS} = 5 \text{ V}$) of $18 \mu\text{S}$, were extracted. The gate current of these devices was typically $< 10^{-11} \text{ A}$. These values are in agreement with other high quality state of the art flexible a-IGZO TFTs [7].

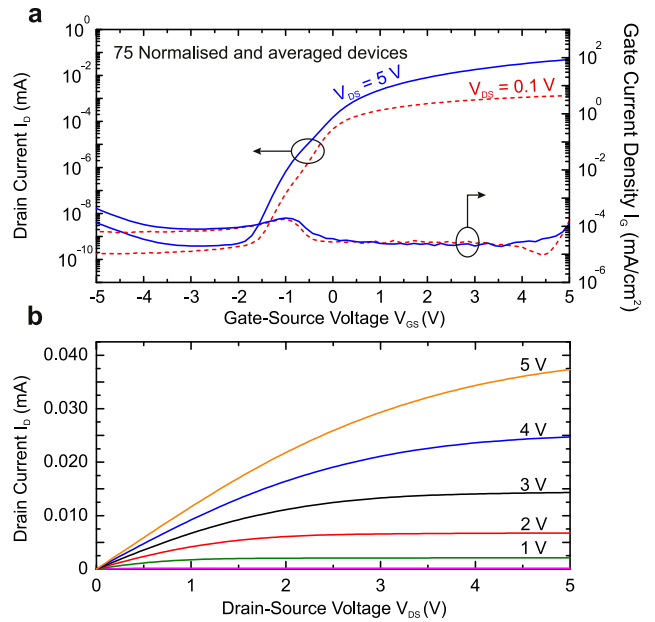


FIGURE 3. TFT characteristics before irradiation, low temperature treatment and magnetic field exposure. **a)** Saturation ($V_{DS} = 5 \text{ V}$) and Linear transfer ($V_{DS} = 0.1 \text{ V}$) curves. **b)** Output curves for Gate Source voltages (V_{GS}) ranging from 0 V to 5 V.

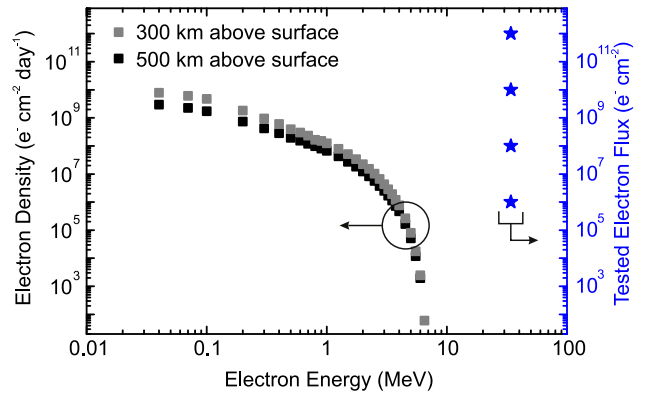


FIGURE 4. Trapped electron density at 300 km and 500 km above Earth's surface as extracted from [3], and electron fluxes tested.

B. ELECTRON IRRADIATION EFFECTS

The TFTs were exposed to electron irradiation with fluence ranging from $10^6 \text{ e}^-/\text{cm}^2$ to $10^{12} \text{ e}^-/\text{cm}^2$. Fig. 4 shows the typical trapped electron densities at 300 km and 500 km for electron energies ranging from 0.04 eV to 6.5 eV. In Fig. 4 the star-shaped points indicate the energy and densities used in this work, which exceed both the density and energies typically existent in LEO. Fig. 5a presents the averaged transfer curves from the same 25 transistors measured before and after exposure to electron irradiation at $10^{12} \text{ e}^-/\text{cm}^2$. The gate current is normalized. From these measurements, a V_{th} shift of $+(0.09 \pm 0.05) \text{ V}$ was observed, whereas the μ_{FE} decreased by $(-5 \pm 6) \%$. The variation of S was observed to be negligible. The I_{ON}/I_{OFF} ratio and the gate current were virtually unaffected by the electron irradiation, remaining at

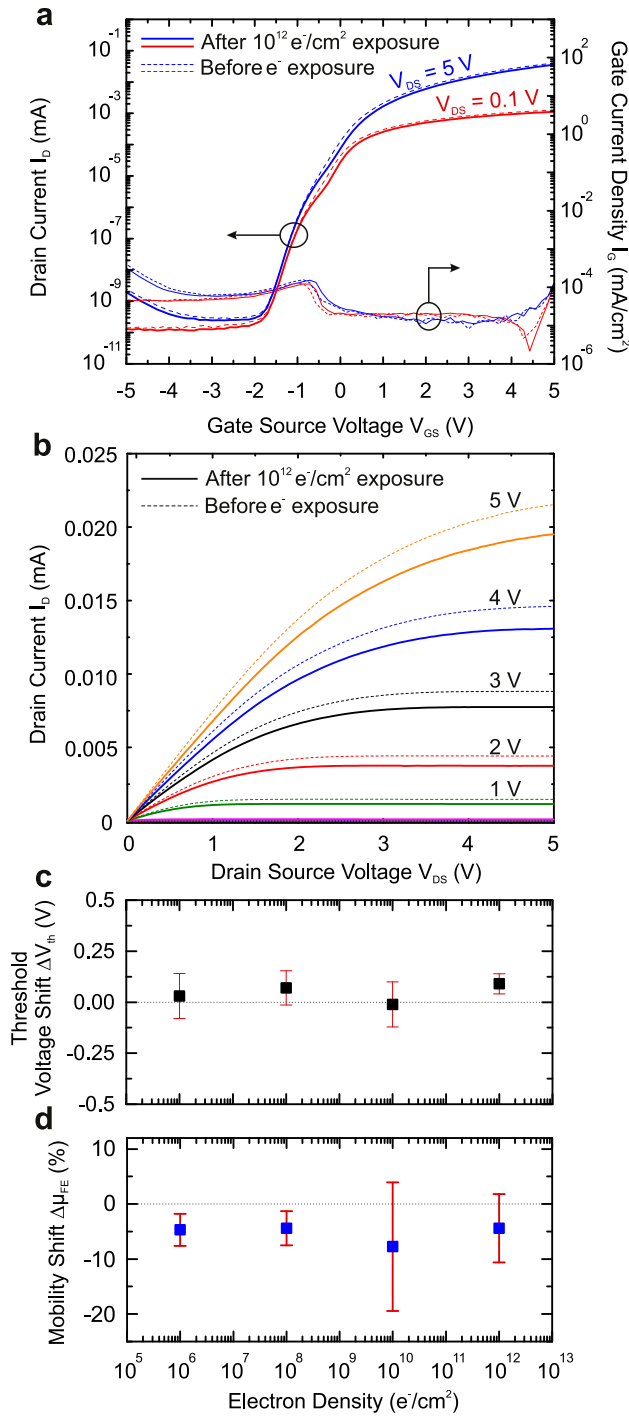


FIGURE 5. Impact of electron irradiation. **a,b)** Averaged transfer and output curves from 25 a-IGZO TFTs exposed to electron irradiation with a density of 10^{12} e⁻/cm². **c,d)** Evolution of the V_{th} and the μ_{FE} for all electron irradiation densities.

10^7 and $<10^{-11}$ A, indicating that the Al_2O_3 gate insulator was not damaged. Fig. 5b shows the averaged output curves for the same transistors, reflecting the decrease in the maximum I_D due to the increase of V_{th} and the decrease of μ_{FE} . Electron irradiation has no impact on the quality of

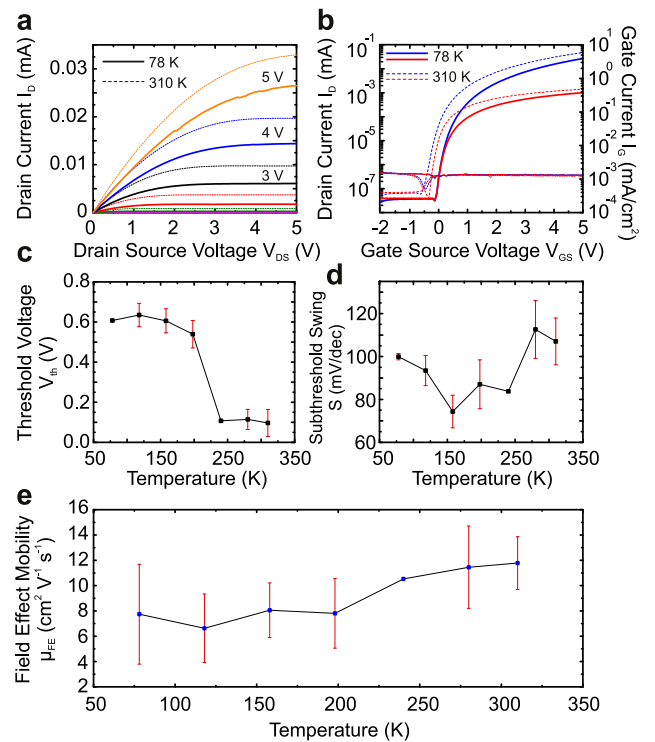


FIGURE 6. Low temperature measurements from a total of 16 transistors. **a)** Output curves at 78 K and 310 K. **b)** Transfer curves. **c,d,e)** V_{th} , S and μ_{FE} variation for temperatures from 78 K to 310 K.

the drain and source contacts, given that no current crowding effects are observed for low V_{DS} [28]. The evolutions of both the V_{th} and μ_{FE} are shown in Figs. 5c and 5d, respectively, with increasing electron irradiation. Parameter extraction was performed before and after irradiation on the same set of transistors (25 TFTs for each electron irradiation density). The threshold voltage is demonstrated to be virtually independent of the electron irradiation, whereas the mobility decreases after irradiation. The shift in V_{th} is significantly smaller than the 1 V V_{th} shift observed for top-gate Al_2O_3 (200 nm) gate dielectric rigid a-IGZO TFTs exposed to 0.8 MeV electrons with a fluence of 10^{14} e⁻/cm², which can be explained by the reduced interaction of the electrons with the low-density polymer substrate. Additionally, it is observed that the shifts magnitude of the mobility is independent of the irradiation fluence. The observed decrease of both I_D and μ_{FE} , as well as the increase of V_{th} can be explained by the formation of both oxygen interstitial and zinc vacancy acceptor defects, caused by the exposition to high energy electrons, as well as by charge trapping at the gate/dielectric [29], [30].

C. LOW TEMPERATURE MEASUREMENTS

Next, the impact of low temperature on flexible a-IGZO transistors was investigated. Fig. 6 shows the averaged performance variation of the characterised transistors. Characteristic curves were extracted from 16 transistors. The

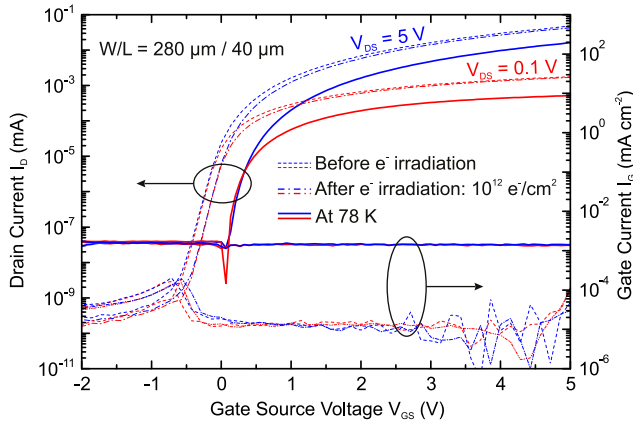


FIGURE 7. Evolution of the saturation and linear transfer curves for a transistor irradiated with the highest electron density, followed by exposure to 78 K.

reduced number of measurements is because the temperature-induced expansion of the polyimide substrate complicated reliable contacting of the devices, and different transistors had to be measured for each temperature. Fig. 6a shows the averaged output curves for the measured transistors, where a decrease of the drain current is observed for 78 K in comparison to the values observed at 310 K. This is explained by the decrease of the thermal energy available for the thermal activation of electrons trapped in defect sites. As it was observed for the irradiated transistors, no current crowding effect is visible for low V_{DS} values. An average V_{th} of 0.6 V with minimal error was extracted from the measured TFTs at 78 K (Fig. 6b), corresponding to a positive shift of (0.51 ± 0.07) V when compared to the (0.09 ± 0.07) V extracted from the same devices at room temperature. The evolution of V_{th} , S and μ_{FE} are presented in Figs. 6c, 6d and 6e, respectively. V_{th} increases for lower temperatures, whereas the subthreshold swing and μ_{FE} decrease for the same interval. The performance of the devices was observed to recover as the temperature returned to 310 K. Previous studies on rigid TFTs have presented similar trends for V_{th} , and μ_{FE} due to the thermal activated profile of a-IGZO [17]. In addition, measurements down to 10 K on rigid a-IGZO TFTs demonstrated that the subthreshold swing increased for temperatures below 80 K [17], which was attributed to a change from band conduction to variable range hopping [31].

D. COMBINED IRRADIATION AND TEMPERATURE

The combined influence of radiation and low temperatures was investigated, Fig. 7 presents the transfer curve evolution of a TFT that was irradiated with $10^{12} e^-/cm^2$ and afterwards cooled down from 310 K to 78 K. As can be seen, in comparison with the devices that were not exposed to electron irradiation, such as the ones on Fig. 6b, the parameter shifts are only slightly affected by the applied electron irradiation. The irradiated sample exhibited V_{th} , μ_{FE} and S shifts of $+0.38$ V, $-5.95 cm^2V^{-1}s^{-1}$ and $+30$ mV/dec, after being cooled down to 78 K. The same parameters shifted by

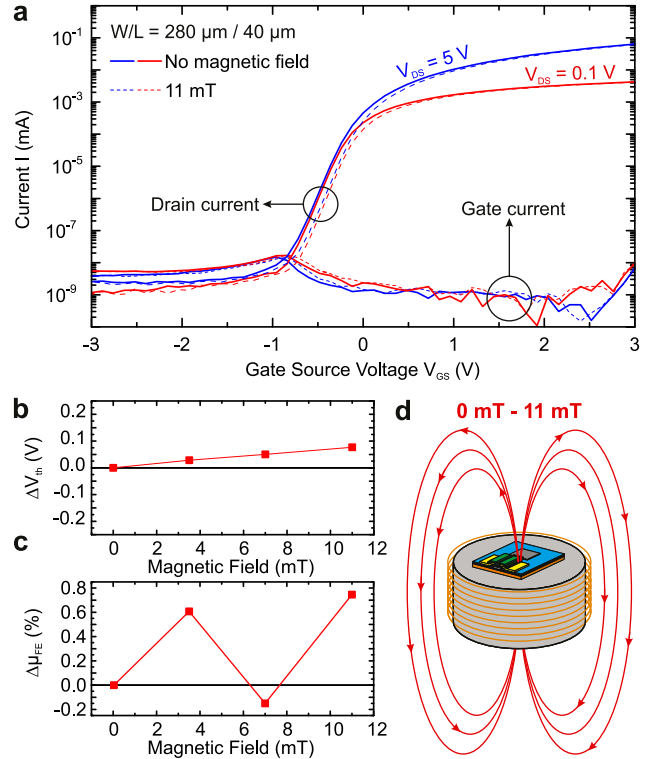


FIGURE 8. Magnetic field effect on a-IGZO flexible TFTs. a) Transfer curves measured at 0 mT (full line) and 11 mT (dashed line). b,c) V_{th} and μ_{FE} shift for a device measured under various magnetic fields. d) Schematic of the setup used to apply the magnetic field.

$+0.13$ V, $-5 cm^2V^{-1}s^{-1}$ and 21 mV/dec for the non irradiated sample. The irradiated sample presents larger parameter shifts at low temperatures. Although these differences are small and could be related to intrinsic performance variations of the samples, the measurement indicates that a combined radiation-temperature effect in flexible a-IGZO TFTs has to be considered for space applications. This combined effect can be caused by an increased number of defects in the irradiated transistors, as high energy electron irradiation has been shown to create acceptor defects on a-IGZO TFTs [14]. The thermally activated occupation and de-occupation of these traps then changes the low temperature behaviour of the TFTs.

E. MAGNETIC FIELD EFFECTS

In addition to the effects of electron irradiation and low temperatures, it is also important to study the influence of magnetic fields on the properties of the devices. Fig. 8a shows the transfer characteristics of a flexible a-IGZO TFT measured at 0 mT and under an 11 mT magnetic field. For comparison, the magnetic field at an altitude of 300 km above the Earth's crust does not typically exceed 20 nT [32]. It has previously been demonstrated that IGZO TFTs can be sensitive to magnetic fields [21]. This sensitivity has nonetheless been correlated with the employed gate insulator. Aoki *et al.* [21] characterised a-IGZO TFTs on glass with both SiN_x and SiO_x gate insulators, which resulted in

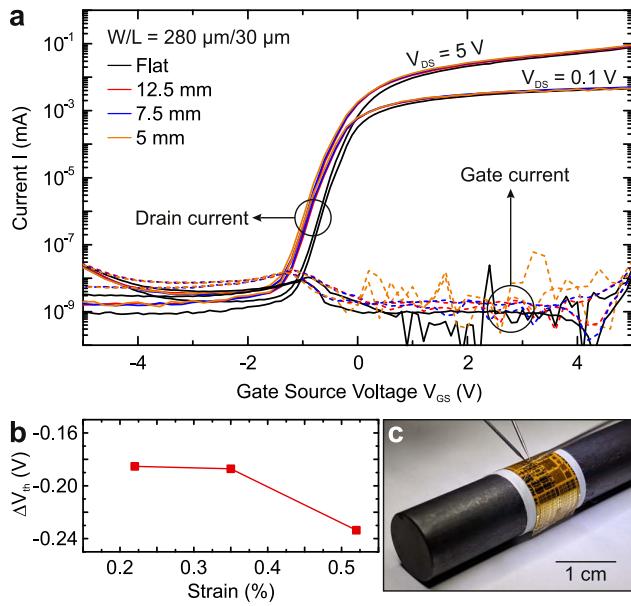


FIGURE 9. Effects of mechanical bending on a-IGZO flexible TFTs. **a)** Transfer curves measured for a flat device and for three different bending radii, 12.5 mm, 7.5 mm and 5 mm. Threshold voltage shift for the various bending radii. **c)** Photograph of bent substrate with measured samples.

conventional (resistance increase) and inverse magnetoresistive effects, respectively. Figs. 8b and 8c show the V_{th} and μ_{FE} of an a-IGZO TFT with Al_2O_3 gate insulator for various magnetic fields. The magnetic field is applied perpendicularly to the direction of the channel (Fig. 8d). This field was generated using a coil wrapped around a ferromagnetic core, and the magnetic field was measured using a Redcliffe 102 Hall magnetometer. The devices were placed on the surface of the ferrite core and in order to exclude the effects of temperature, the core's surface temperature was monitored during the measurements and was not allowed to exceed room temperature (RT) + 1°C. All measurements were conducted in the dark and in a standard atmosphere. Although a 0.08 V positive shift is observed for the V_{th} , this effect was also observed for devices measured repeatedly under a 0 mT magnetic field. Given that the μ_{FE} was not significantly affected by the magnetic field, the V_{th} shift is most probably related with gate bias stressing of the devices. These results show that flexible a-IGZO TFTs can operate under magnetic fields 10^6 times larger than the ones found in LEO [32].

F. DEVICE BENDABILITY

Assessing the flexibility of these devices is important given the desired application in flexible sensors. For this reason, the TFTs were tested under bending at various radii after exposure to electron irradiation, low temperature and magnetic fields. Fig. 9 shows the resulting transfer characteristics under 12.5 mm, 7.5 mm and 5 mm bending radii, corresponding to tensile strains of 0.22 %, 0.35 % and 0.52 % calculated from [33]. The devices were attached to rods as shown in

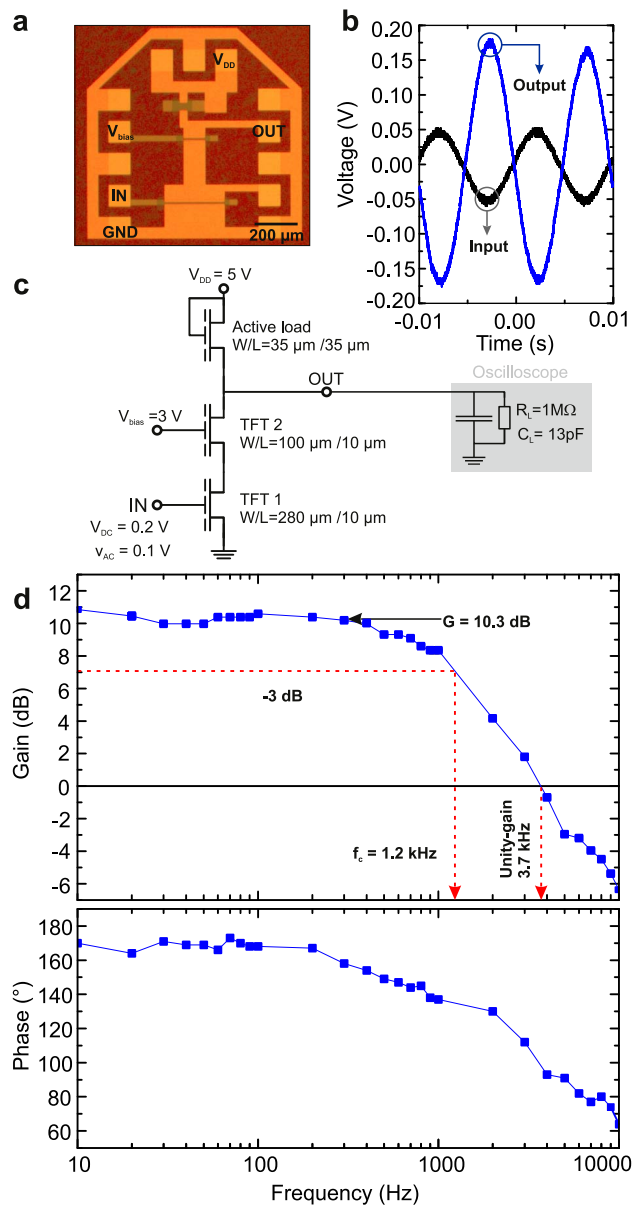


FIGURE 10. Flexible a-IGZO Cascode amplifier. **a)** Micrograph of the integrated circuit. **b)** Representative input and output voltages at $f = 100$ Hz. **c)** Circuit schematic showing the individual TFT dimensions, output load, as well as bias and input voltages. **d)** Bode plot measured after the circuit was exposed to electron irradiation ($10^{12} e^- / cm^2$), low temperatures (78 K), and magnetic fields (11 mT).

Fig. 9c to apply strain parallel to the TFT channel. The transfer curve of the devices shifted in the negative direction with decreasing bending radii, and the exact V_{th} is captured in Fig 9b. Re-flattening the device resulted in a gradual recovery of the transfer curve [34], however, bending to smaller radii causes cracks and permanently damages the devices. In addition, no significant increase of the gate leakage current was measured for all bending radii, indicating that the dielectric layer was not significantly affected by the bending stress. This negative shift is in line with the effect of tensile strain on non irradiated a-IGZO TFTs. These results illustrate the flexibility of the devices studied in this work.

G. INTEGRATED AMPLIFIER

In addition to individual TFTs, the functionality of an integrated circuit was investigated after it was exposed to an electron irradiation of 10^{12} e⁻/cm², temperatures as low as 78 K, and magnetic flux densities up to 11 mT. These represent the most extreme conditions discussed here. Fig. 10a shows a micrograph of the tested voltage amplifier fabricated using three IGZO TFTs, and Fig. 10b shows a representative amplified signal at a frequency of 100 Hz. In addition, Fig. 10c displays the corresponding circuit schematic which also indicates the TFT dimensions, input, bias, and supply voltages, as well as the loading effect of the characterisation equipment. The employed Cascode topology based on standard NMOS design principle utilizes an active load and represents a tradeoff between circuit complexity and performance. This is because the Cascode reduces the Miller effect and hence the negative impact of parasitic overlap capacitance, unavoidable if circuits are fabricated on free-standing flexible substrates [35]. Such amplifiers are essential for the conditioning of a variety of sensors.

Figs. 10b and 10d prove that the circuit is fully functional. After, irradiation, temperature and B-field stress, the Cascode circuit provides an average low frequency voltage gain of 10.3 dB, a -3 dB cutoff frequency of 1.2 kHz, and a unity gain frequency of 3.7 kHz. This results in a gain bandwidth product (GBWP) of 3.6 kHz. Furthermore the Cascode architecture also results in power consumption of only 62.5 μW. Commercial rigid amplifiers such as the OPA277 tested using temperatures down to 73 K have a GBWP of 1 MHz [36]. However, in comparison, flexible amplifier systems using pentacene TFTs show maximum GBWP of 2 kHz and their reliability has not been tested after they've been exposed to conditions similar to the ones found in space [37].

IV. CONCLUSION

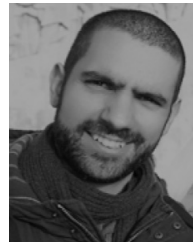
The suitability of flexible a-IGZO TFTs was assessed for the development of electronic devices for conformable and lightweight space applications. Electron irradiation followed by low temperature treatment down to 78 K were conducted to simulate the harsh environment found in Low Earth Orbit. Trap creation caused by electron irradiation induces a positive V_{th} shift and a decrease of the μ_{FE} for electron irradiation densities up to 10^{12} e⁻/cm² and electron energy of 34.1 MeV. Nonetheless, the variation of the electron irradiation fluence did not influence the magnitude of these shifts. Subsequent low temperature measurements down to 78 K resulted in an average decrease of 20% for the μ_{FE} , accompanied by a positive V_{th} shift and a decrease of the subthreshold swing that reached a minimum of 66.5 mV/dec. It was also demonstrated that the temperature induced parameter shifts are slightly influenced by previous electron irradiation. Regarding the magnetic field impact on the performance of the TFTs, no visible variation was observed. Finally, a Cascode amplifier was shown to be operational after the sample had been irradiated and exposed to low temperatures and magnetic fields that exceeded the

conditions found in Low Earth Orbit. These results show that a-IGZO TFTs fabricated on flexible polyimide substrates are a viable option for the development of lightweight and unobtrusive devices for space applications, such as smart textiles for space suits.

REFERENCES

- [1] T. Dachev, W. Atwell, E. Semones, B. Tomov, and B. Reddell, "Observations of the SAA radiation distribution by Liulin-E094 instrument on ISS," *Adv. Space Res.*, vol. 37, no. 9, pp. 1672–1677, 2006. [Online]. Available: <https://doi.org/10.1016/j.asr.2006.01.001>
- [2] F. J. Pavón-Carrasco and A. De Santis, "The south atlantic anomaly: The key for a possible geomagnetic reversal," *Front. Earth Sci.*, vol. 4, p. 40, Mar. 2016. [Online]. Available: <https://doi.org/10.3389/feart.2016.00040>
- [3] E. G. Stassinopoulos and J. P. Raymond, "The space radiation environment for electronics," *Proc. IEEE*, vol. 76, no. 11, pp. 1423–1442, Nov. 1988. [Online]. Available: <https://doi.org/10.1109/5.90113>
- [4] L. Basiricò *et al.*, "Space environment effects on flexible, low-temperature organic thin-film transistors," *ACS Appl. Mater. Interfaces*, vol. 9, no. 40, pp. 35150–35158, Sep. 2017. [Online]. Available: <https://doi.org/10.1021/acsami.7b08440>
- [5] M. Kagan, V. Nadorov, S. Guha, J. Yang, and A. Banerjee, "Space qualification of amorphous silicon alloy lightweight modules," in *Proc. Conf. Rec. 28th IEEE Photovoltaic Specialists*, 2000, pp. 1261–1264. [Online]. Available: <https://doi.org/10.1109/pvsc.2000.916119>
- [6] K. Nomura, H. Ohta, A. Takagi, T. Kamiya, M. Hirano, and H. Hosono, "Room-temperature fabrication of transparent flexible thin-film transistors using amorphous oxide semiconductors," *Nature*, vol. 432, no. 7016, p. 488, 2004. [Online]. Available: <https://doi.org/10.1038/nature03090>
- [7] L. Petti *et al.*, "Metal oxide semiconductor thin-film transistors for flexible electronics," *Appl. Phys. Rev.*, vol. 3, no. 2, 2016, Art. no. 021303. [Online]. Available: <https://doi.org/10.1063/1.4953034>
- [8] J. K. Jeong, H. W. Yang, J. H. Jeong, Y.-G. Mo, and H. D. Kim, "Origin of threshold voltage instability in indium-gallium-zinc oxide thin film transistors," *Appl. Phys. Lett.*, vol. 93, no. 12, 2008, Art. no. 123508. [Online]. Available: <https://doi.org/10.1063/1.2990657>
- [9] K. Ide, K. Nomura, H. Hosono, and T. Kamiya, "Electronic defects in amorphous oxide semiconductors: A review," *Physica Status Solidi (a)*, vol. 216, no. 5, 2019, Art. no. 1800372. [Online]. Available: <https://doi.org/10.1002/pssa.201800372>
- [10] J. C. Costa, A. Wishahi, A. Pouryazdan, M. Nock, and N. Münzenrieder, "Hand-drawn resistors, capacitors, diodes, and circuits for a pressure sensor system on paper," *Adv. Elect. Mater.*, vol. 4, no. 5, 2018, Art. no. 1700600. [Online]. Available: <https://doi.org/10.1002/aelm.201700600>
- [11] M. Nag *et al.*, "Flexible amoled display and gate-driver with self-aligned IGZO TFT on plastic foil," in *SID Symp. Dig. Tech. Papers*, vol. 45, no. 1, 2014, pp. 248–251. [Online]. Available: <https://doi.org/10.1002/j.2168-0159.2014.tb00068.x>
- [12] D. Karnausenko *et al.*, "Biomimetic microelectronics for regenerative neuronal cuff implants," *Adv. Mater.*, vol. 27, no. 43, pp. 6797–6805, 2015. [Online]. Available: <https://doi.org/10.1002/adma.201503696>
- [13] P. G. Bahubalindrani *et al.*, "Analog circuits with high-gain topologies using a-GIZO TFTS on glass," *J. Display Technol.*, vol. 11, no. 6, pp. 547–553, 2015. [Online]. Available: <https://doi.org/10.1109/JDT.2014.2378058>
- [14] H. J. Moon, S. H. Jung, M. K. Ryu, K. I. Cho, E.-J. Yun, and B. S. Bae, "Effect of high-energy electron beam irradiation on the gate-bias stability of IGZO TFTs," *J. Korean Phys. Soc.*, vol. 60, no. 2, pp. 254–260, 2012. [Online]. Available: <https://doi.org/10.3938/jkps.60.254>
- [15] S. A. Tijani, Y. Al-Hadeethi, I. Sambo, and F. A. Balogun, "Shielding of beta and bremsstrahlung radiation with transparent bi₂O₃-b₂O₃-TeO₂ glasses in therapeutic nuclear medicine," *J. Radiol. Protect.*, vol. 38, no. 3, pp. N44–N51, Aug. 2018. [Online]. Available: <https://doi.org/10.1088/1361-6498/aad2be>

- [16] J. Marczewski *et al.*, "Monolithic silicon pixel detectors in SOI technology," *Nucl. Instrum. Methods Phys. Res. A Accelerators Spectrometers Detect. Assoc. Equip.*, vol. 549, nos. 1–3, pp. 112–116, Sep. 2005. [Online]. Available: <https://doi.org/10.1016/j.nima.2005.04.035>
- [17] M. D. H. Chowdhury, P. Migliorato, and J. Jang, "Low temperature characteristics in amorphous indium–gallium–zinc–oxide thin-film transistors down to 10 K," *Appl. Phys. Lett.*, vol. 103, no. 15, 2013, Art. no. 152103. [Online]. Available: <https://doi.org/10.1063/1.4824875>
- [18] G. Schwarz, "Thermal expansion of polymers from 4.2k to room temperature," *Cryogenics*, vol. 28, no. 4, pp. 248–254, Apr. 1988. [Online]. Available: [https://doi.org/10.1016/0011-2275\(88\)90009-4](https://doi.org/10.1016/0011-2275(88)90009-4)
- [19] C. Scherer, J. Horbach, F. Schmid, and M. Letz, "Negative thermal expansion of quartz glass at low temperatures: An AB initio simulation study," *J. Non Crystalline Solids*, vol. 468, pp. 82–91, Jul. 2017. [Online]. Available: <https://doi.org/10.1016/j.jnoncrysol.2017.04.035>
- [20] N. Münzenrieder, L. Petti, C. Zysset, T. Kinkeldei, G. A. Salvatore, and G. Tröster, "Flexible self-aligned amorphous ingazno thin-film transistors with submicrometer channel length and a transit frequency of 135 MHz," *IEEE Trans. Electron Devices*, vol. 60, no. 9, pp. 2815–2820, Sep. 2013. [Online]. Available: <https://doi.org/10.1109/TED.2013.2274575>
- [21] K. Aoki *et al.*, "Magnetoresistive effect of amorphous In-Ga-Zn-O magnetic field sensors," *IEEE Electron Device Lett.*, vol. 38, no. 8, pp. 1143–1145, Aug. 2017. [Online]. Available: <https://doi.org/10.1109/LED.2017.2721422>
- [22] J. G. Funk and G. F. Sykes, Jr., "The effects of simulated space environmental parameters on six commercially available composite materials," *Nat. Aeronautics Space Admin.*, Hampton, VA, USA, Rep. NASA-TP-2906, 1989.
- [23] W. S. Wong and A. Salleo, Eds., *Flexible Electronics*. New York, NY, USA: Springer, 2009. [Online]. Available: <https://doi.org/10.1007/978-0-387-74363-9>
- [24] F. Gabriel *et al.*, "The Rossendorf radiation source ELBE and its FEL projects," *Nucl. Instrum. Methods Phys. Res. B Beam Interact. Mater. Atoms*, vol. 161, pp. 1143–1147, Mar. 2000. [Online]. Available: [https://doi.org/10.1016/S0168-583X\(99\)00909-X](https://doi.org/10.1016/S0168-583X(99)00909-X)
- [25] "The use of parallel ionization chambers in high energy electron and photon beams," *Int. Atomic Energy Agency*, Vienna, Austria, Rep. TRS-381, 1997.
- [26] J. R. Young, "Penetration of electrons and ions in aluminum," *J. Appl. Phys.*, vol. 27, no. 1, pp. 1–4, Jan. 1956. [Online]. Available: <https://doi.org/10.1063/1.1722186>
- [27] H. Shichman and D. A. Hodges, "Modeling and simulation of insulated-gate field-effect transistor switching circuits," *IEEE J. Solid-State Circuits*, vol. SSC-3, no. 3, pp. 285–289, Sep. 1968. [Online]. Available: <http://doi.org/10.1109/JSSC.1968.1049902>
- [28] K. Takechi, M. Nakata, T. Eguchi, H. Yamaguchi, and S. Kaneko, "Study on current crowding in the output characteristics of amorphous ingazno4 thin-film transistors using dual-gate structures with various active-layer thicknesses," *Jpn. J. Appl. Phys.*, vol. 48, no. 8, 2009, Art. no. 081606. [Online]. Available: <https://doi.org/10.1143/JJAP.48.081606>
- [29] S. H. Jeong, B. S. Bae, K. M. Yu, M. K. Ryu, K. I. Cho, and E.-J. Yun, "Properties of IGZO thin films irradiated by electron beams with various energies," *J. Korean Phys. Soc.*, vol. 61, no. 6, pp. 867–872, 2012. [Online]. Available: <https://doi.org/10.3938/jkps.61.867>
- [30] G. K. Dayananda, C. S. Rai, A. Jayarama, and H. J. Kim, "Study of radiation resistance property of a-IGZO thin film transistors," in *Proc. IEEE Int. Conf. Recent Trends Electron. Inf. Commun. Technol. (RTEICT)*, 2016, pp. 1816–1819. [Online]. Available: <https://doi.org/10.1109/RTEICT.2016.7808148>
- [31] J. Jeong, G. J. Lee, J. Kim, S. M. Jeong, and J.-H. Kim, "Analysis of temperature-dependent electrical characteristics in amorphous inga-zn-o thin-film transistors using gated-four-probe measurements," *J. Appl. Phys.*, vol. 114, no. 9, 2013, Art. no. 094502. [Online]. Available: <https://doi.org/10.1063/1.4819886>
- [32] N. Olsen *et al.*, "CHAOS—A model of the earth's magnetic field derived from CHAMP, Ørsted, and SAC-C magnetic satellite data," *Geophys. J. Int.*, vol. 166, no. 1, pp. 67–75, Jul. 2006. [Online]. Available: <https://doi.org/10.1111/j.1365-246x.2006.02959.x>
- [33] H. Gleskova, S. Wagner, and Z. Suo, "A-Si:H thin film transistors after very high strain," *J. Non Crystalline Solids*, vols. 266–269, pp. 1320–1324, May 2000. [Online]. Available: [https://doi.org/10.1016/S0022-3093\(99\)00944-8](https://doi.org/10.1016/S0022-3093(99)00944-8)
- [34] N. Munzenrieder, K. H. Cherenack, and G. Troster, "The effects of mechanical bending and illumination on the performance of flexible IGZO TFTs," *IEEE Trans. Electron Devices*, vol. 58, no. 7, pp. 2041–2048, Jul. 2011. [Online]. Available: <https://doi.org/10.1109/ted.2011.2143416>
- [35] N. Münzenrieder *et al.*, "Flexible a-IGZO TFT amplifier fabricated on a free standing polyimide foil operating at 1.2 MHz while bent to a radius of 5 mm," in *Proc. Int. Electron Devices Meeting*, 2012, pp. 2–5. [Online]. Available: <https://doi.org/10.1109/IEDM.2012.6478982>
- [36] M. Song, J. Y. Yang-Scharlotta, M. Ashtijou, and M. Mojarradi, "Evaluation of commercial-off-the-shelf (COTS) electronics for extreme cold environments," in *Proc. IEEE Aerosp. Conf.*, Mar. 2018, pp. 1–12. [Online]. Available: <https://doi.org/10.1109/aero.2018.8396695>
- [37] H. Marien, M. Steyaert, E. van Veenendaal, and P. Heremans, "DC–DC converter assisted two-stage amplifier in organic thin-film transistor technology on foil," in *Proc. ESSCIRC*, Sep. 2011, pp. 411–414. [Online]. Available: <https://doi.org/10.1109/essirc.2011.6044994>



JÚLIO C. COSTA received the M.Sc. degree in micro and nanotechnologies from the New University of Lisbon, Lisbon, Portugal, in 2015. He is currently pursuing the Ph.D. degree with the University of Sussex, Brighton, U.K. His current research interests include flexible electronics, biosensors, and wearables.



ARASH POURYAZDAN received the B.Eng. degree in electrical and electronic engineering and the Ph.D. degree in electrical engineering from the University of Sussex, Brighton, U.K. in 2013 and 2018, respectively. His current research interests include noncontact electric potential sensing and microscopy, novel flexible sensors, wearable electronics, and innovative acoustic interfaces.



JULIANNA PANIDI received the B.Sc. degree in material science from the University of Patras and the M.Res. degree from the University Pierre et Marie Curie Paris, France, before moving to Imperial College London, where she joined the Plastic Electronics CDT for an M.Res. and Ph.D. in Prof. Thomas D. Anthopoulos's Group.



FILIPPO SPINA (S'19) received the B.Sc. degree in computer engineering from Roma Tre University in 2007, and the M.Sc. degree in robotics and autonomous systems from the University of Sussex, Brighton, U.K., in 2017, where he is currently pursuing the Ph.D. degree. His major interest is the monolithic production through additive manufacturing technologies, feedback control, and hardware/software integration of soft biomimetic actuators with embedded sensors.



THOMAS D. ANTHOPOULOS received the B.Eng. and D.Phil. degrees from Staffordshire University, U.K., followed by post-doctoral appointments with the University of St. Andrews, U.K., and Philips Research Laboratories, The Netherlands, before moving to a faculty position with Imperial College London, U.K., in 2006. In 2017, he joined the King Abdullah University of Science and Technology, Saudi Arabia, where he is a Professor of material science and engineering.



ANDREAS WAGNER received the Ph.D. degree in physics from Technical University Darmstadt, Germany, in 1996. He was with GSI-Helmholtzzentrum für Schwerionenforschung from 1996 to 1997, and with the National Superconducting Cyclotron Laboratory, Michigan State University, East-Lansing, MI, USA, from 1997 to 1999. He is the Head of the Nuclear Physics Division, Helmholtz-Zentrum Dresden-Rossendorf (HZDR), Germany. He has over 250 authored/coauthored papers covering fundamental nuclear physics, detector developments, and materials research with positrons. He is leading the scientific programs at several end stations of the superconducting electron linear accelerator ELBE with HZDR.



MACIEJ O. LIEDKE received the Ph.D. degree in physics from the Technical University of Kaiserslautern, Germany, in 2007. He is a Beamline Scientist at the positron source of the electron linac for beams with high brilliance and low emittance (EPOS-ELBE) with the Institute of Radiation Physics and a Staff Member of the Nuclear Physics Division, Helmholtz-Zentrum Dresden-Rossendorf, Germany. He has over 50 authored/coauthored papers covering magnetism and materials research.



CHRISTOF SCHNEIDER received the B.Sc. degree from the University of Ulm, Germany, in 1986, the Diploma degree in high energy physics from the University of Heidelberg in 1990, and the Ph.D. degree in meson physics from the Technical University of Dresden in 1997. He was a Post-Doctoral Fellow of meson physics with Forschungszentrum Dresden in 1997. Since 2001, he has been with ELBE-Accelerator, Helmholtz-Zentrum Dresden-Rossendorf.



NIKO MÜNZENRIEDER (S'11–M'14) received the Diploma degree in physics from Technische Universität München, Munich, Germany, in 2008, and the Ph.D. degree in electrical engineering from ETH Zurich, Zürich, Switzerland, in 2013. He joined the University of Sussex, Brighton, U.K., as a (Senior) Lecturer leading the Flexible Electronics Laboratory. He is currently an Associate Professor with the Free University of Bozen-Bolzano, Bozen, Italy, researching on thin-film oxide electronics, smart textiles, and flexible sensor systems.